

Results

Without knowing the exact algorithm and sets of initial conditions used by Hastings and Powell in order to solve the ordinary differential equations (Eq. 9-12), we were able to replicate their main findings. First, our time series of the nondimensional variables (fig. 1 (a-c)) present similar patterns as those identified by Hastings and Powell. We observed that the standardized population densities of X, Y, and Z (Eq. 5-7) oscillate in a period of around 125 time steps. In a cycle, the population densities of species X and Y oscillate while that of species Z grows. At the point where z reaches its local maximum, defined above (see methods) as its maximum value within the cycle, and where y and x reach their local minimum and maximum values, respectively, z declines until it reaches its local minimum. This is the “handle” of the teacup (fig. 1 (d)). Subsequently, another cycle begins. We produced an animated figure that illustrates this dynamic (see supp. online material). Furthermore, the discrepancies between our results and those of Hastings and Powell don’t seem to strongly influence the above-mentioned period length, nor the values of the local maxima and minima of our dimensionless variables. Indeed, x varies approximately from 0.2 to 1.0, y from 0.0 to 0.4, and z from 7.5 to 10.5, as seen in the time interval shown in fig. 1 (b₁ = 3.0). The difference in shapes of the phase plots are mainly due to the choices of axis tick intervals and to the angles of the three-dimensional plots.

Second, the first values of the time series of x (fig. 2) are almost identical to those of Hastings and Powell approximately until $t = 250$. Beyond this threshold, the trajectories seem to increasingly diverge from those of the authors. This is not surprising since the initial conditions we used ($x = 0.77$: solid line ; $x = 0.78$: dash line) were distinct, although similar, to the ones used by Hastings and Powell, which were not mentioned in their article. This further supports the chaotic behaviour of the model system where different initial conditions ultimately lead to different trajectories.

Third, our bifurcation diagrams (fig. 3) have the same general shapes as the ones of Hastings and Powell, and are in the same range of z_{\max} . We identified most of the local maxima of z found by the authors for b_1 ranging from 2.2 to 6.5. However, we missed some of them and found others that were absent in their paper. For instance, for $b_1 = 3.1$, we found multiple local maxima of z, whereas the original authors found a dichotomy. The differences are nevertheless more apparent in fig. 3 (c), which represents a detailed portion of fig. 3 (a). For example, inconsistent with the findings of Hastings and Powell, we identified local maxima for b_1 ranging from 2.30 and 2.35. In other words, they found a significant gap in their bifurcation diagram that we did not observe.

Lastly, although Hastings and Powell did not specify the equation of the plane that crosses the trajectories of the phase plot at its “handle”, we were able to accurately replicate their Poincaré section and map for $b_1 = 3.0$ (fig. 4 (a, b)). The main discordance lies in the number of points that cross the plane, and consequently on the apparent smoothness of the graphs. On the contrary, it was harder to precisely replicate the Poincaré map for $b_1 = 6.0$ (fig. 4 (d)), even though the corresponding reproduced Poincaré section (fig. 4 (c)) was similar to the one in Hastings and Powell’s paper.

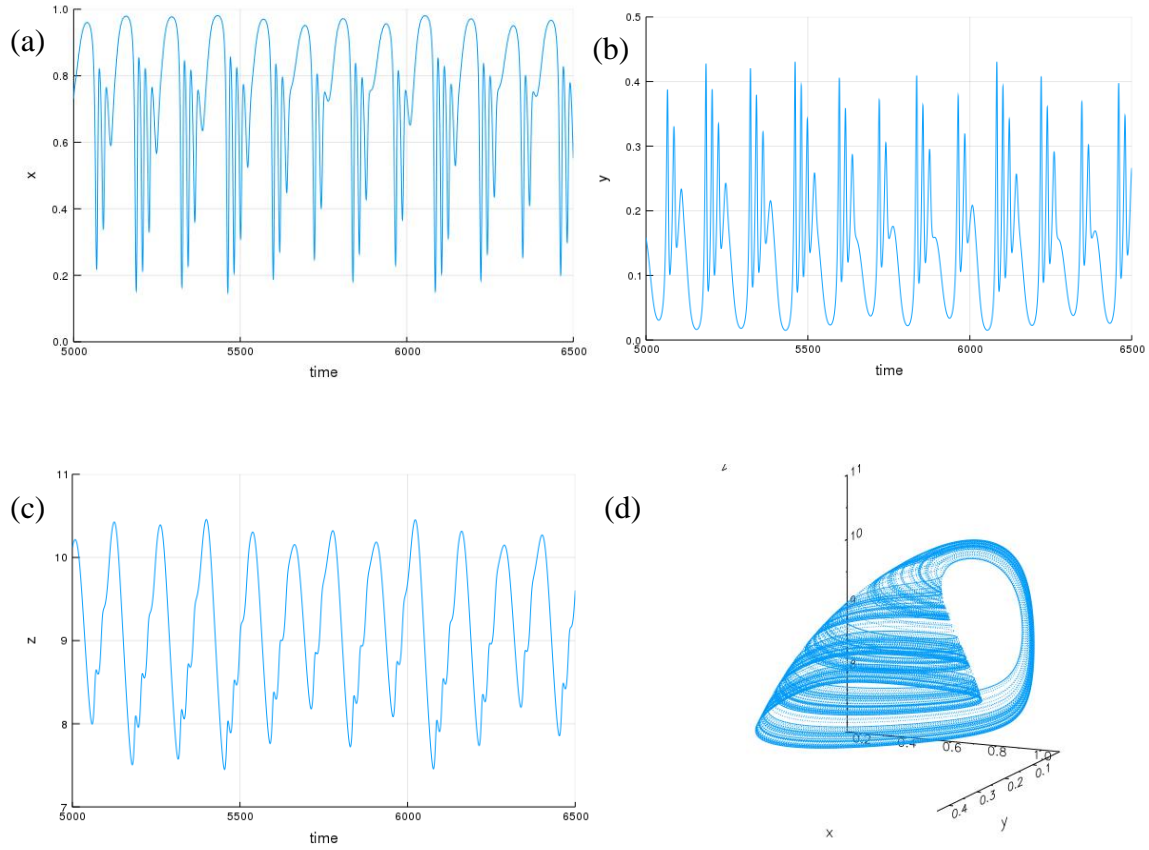


Figure 1: Time series of the nondimensional variables (a) x , (b) y and (c) z , for t ranging from 5000 to 6500 ($x = 1.0$, $y = 1.0$, and $z = 1.0$ as initial conditions). (d) Three-dimensional phase plot, for t ranging from 1 to 10000 ($x = 0.7$, $y = 0.2$, and $z = 8.0$ as initial conditions). The parameter values used in the simulations are given in Table 1 ($b_1 = 3.0$). This figure replicates fig. 2 of Hastings and Powell.

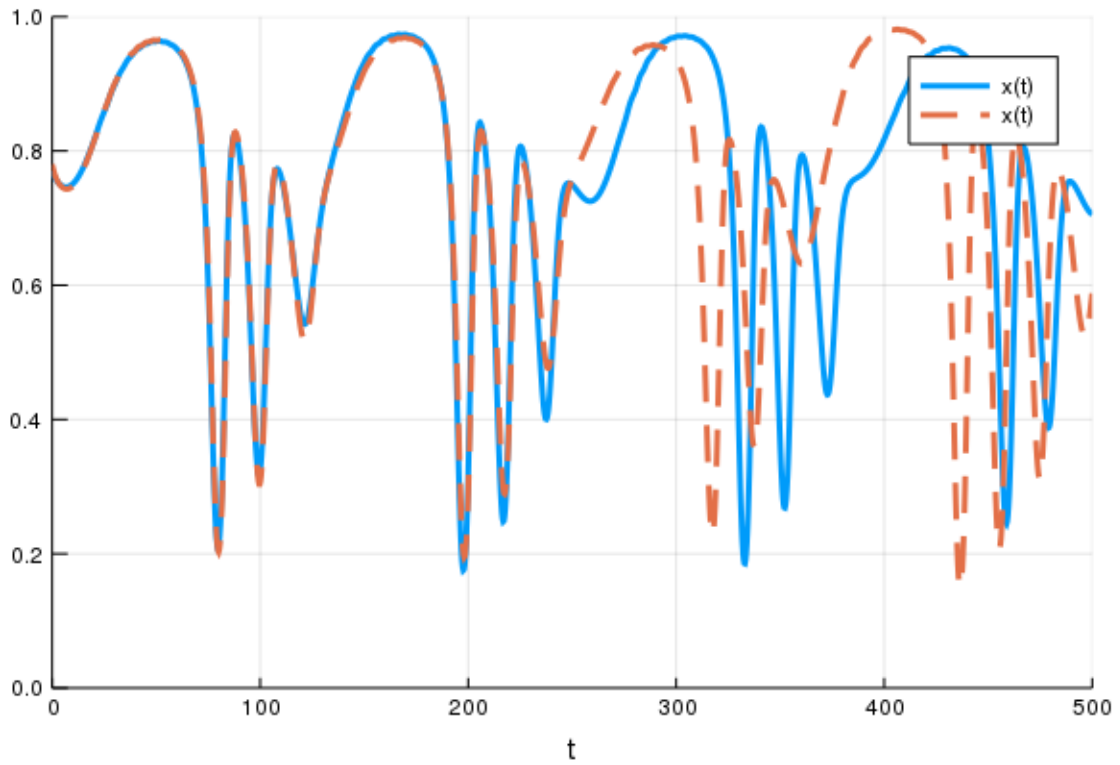


Figure 2: Time series of x , for t ranging from 0 to 500. The solid and dash lines have $x = 0.77$ and $x = 0.78$ as initial conditions, respectively ($y = 0.16$ and $z = 9.9$ as initial conditions are unchanged). The parameter values used in the simulations are given in Table 1 ($b_1 = 3.0$). This figure replicates fig. 3 of Hastings and Powell.

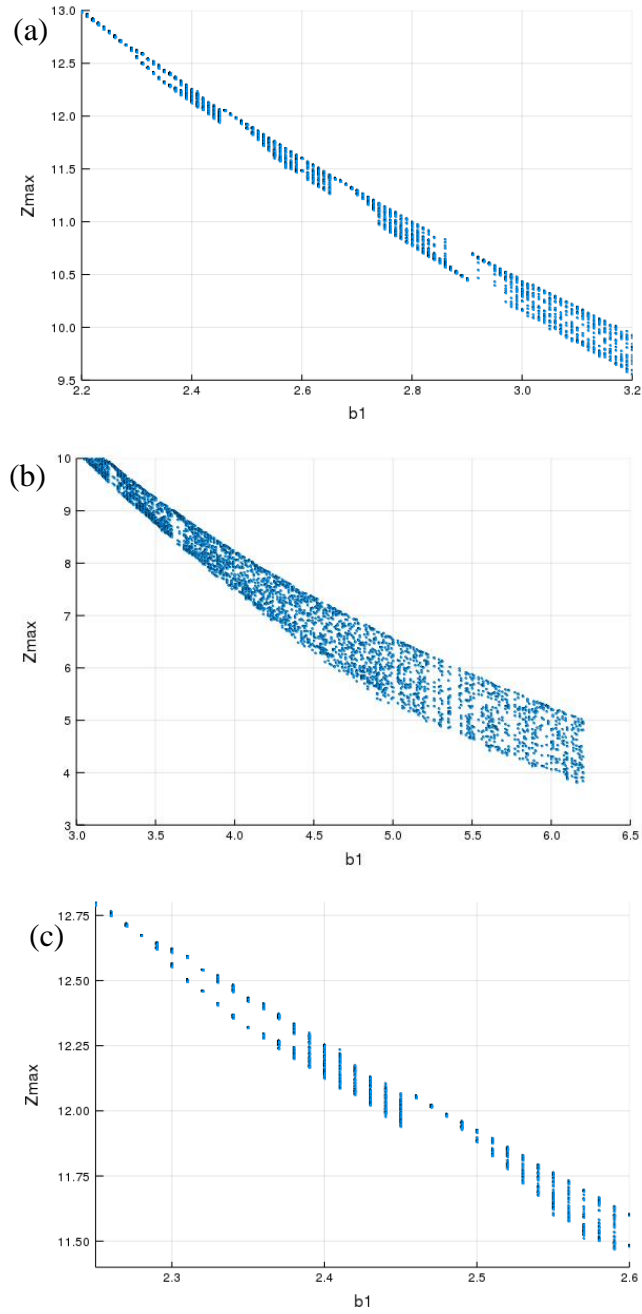


Figure 3: Bifurcation diagrams of the local maxima of z plotted against b_1 which ranges from (a) 2.2 to 3.2, (b) 3.0 to 6.5, and (c) 2.25 to 2.6. The other parameter values used in the simulations are given in Table 1 ($x = 1.0$, $y = 1.0$, and $z = 1.0$ as initial conditions). This figure replicates fig. 4 of Hastings and Powell.

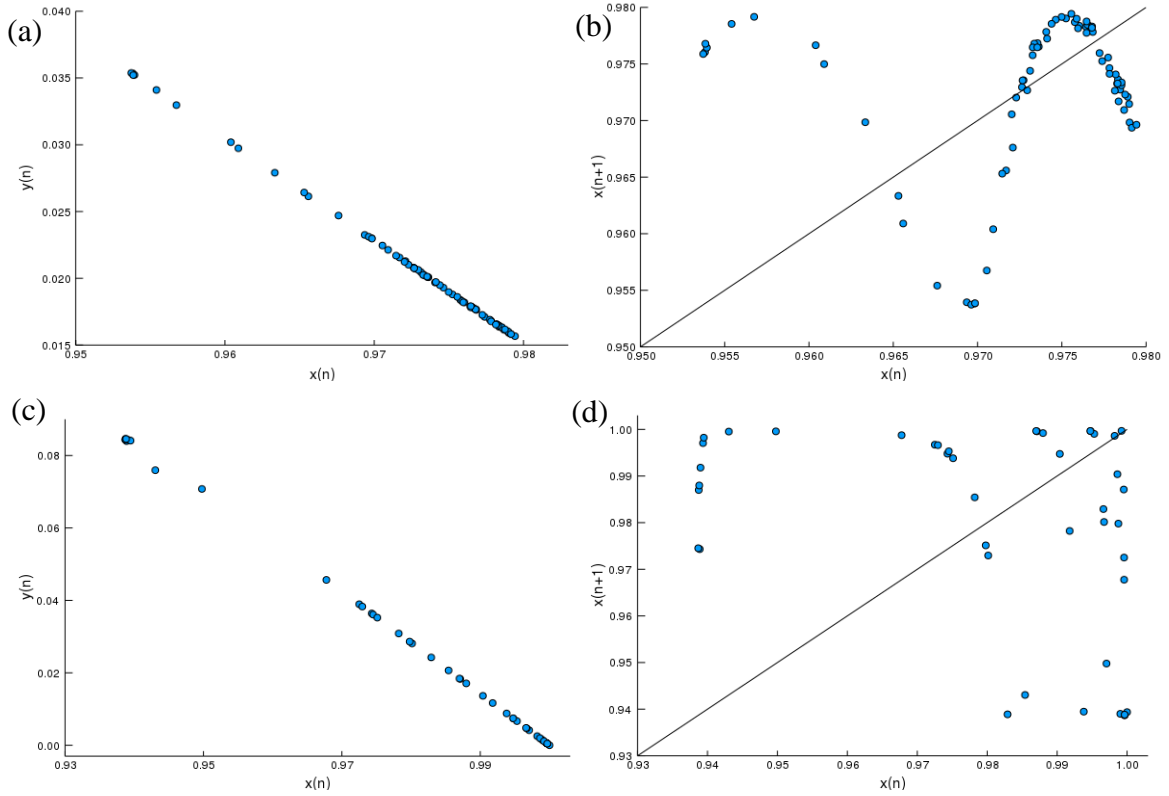


Figure 4: (a) and (b) Poincaré section and map, respectively, for the parameter values given in Table 1 ($b_1 = 3.0$). (c) and (d) Poincaré section and map, for the same parameter values, except $b_1 = 6.0$. All sets of initial values are unchanged ($x = 0.7$, $y = 0.2$, $z = 8.0$). The solid lines of equation $x(n+1) = x(n)$ are shown in (b) and (d). This figure replicates fig. 5 of Hastings and Powell, except their fig. 5 (E), which is partly reproduced in our fig. 2 (d).